

Supporting Information

Ferromagnetically Coupled Chiral Cyanide-bridged $\{\text{Ni}_6\text{Fe}_4\}$ Cages

Takuya Shiga, Graham N. Newton, Jennifer S. Mathieson, Tamaki
Tetsuka, Masayuki Nihei, Leroy Cronin and Hiroki Oshio*

Dr. T. Shiga, Dr. G. N. Newton, T. Tetsuka, Dr. M. Nihei and Prof. H. Oshio
Graduate School of Pure and Applied Sciences,
University of Tsukuba
Tennodai 1-1-1, Tsukuba, Ibaraki 305-8571 (Japan)
Fax: +81-29-852-5923; Tel: +81-29-852-5923
E-mail: oshio@chem.tsukuba.ac.jp

J. S. Mathieson and Prof. L. Cronin
WestCHEM, Department of Chemistry,
The University of Glasgow,
University Avenue, Glasgow, G12 8QQ, UK.
Fax: +44-141-330-4888; Tel: +44-141-330-6650
E-mail: L.Cronin@chem.gla.ac.uk.

Additional Experimental Information

UV/VIS absorption spectra were measured between 200 and 1200 nm with a Shimadzu UV-vis spectrometer UV-3100.

CD spectra for the acetonitrile solutions and KCl pellets were recorded on a JASCO J-810 spectropolarimeter. The measurements of acetonitrile solutions were in the range of 1100-700 nm and 900-220 nm and were performed using the bandwidths of 2 nm and 1 nm, respectively. The measurements on KCl were in the range of 1000-700 nm and 900-245 nm with bandwidths of 10 nm and 4 nm, respectively. 10% diluted KCl pellets were measured in the range of 500-190 nm, with a bandwidth of 4 nm.

Cryospray measurements at -20 °C were carried out at concentrations of the complex in the region of 10^{-5} mol L⁻¹ in methanol using a Bruker microTOFQ instrument. Data was collected in positive ion mode and the spectrometer was previously calibrated with the standard tune mix to give a precision of ca. 1.5 ppm in the region of 500-3000 m/z. The standard parameters for a medium mass data acquisition were used, the end plate voltage was set to -500 V and the capillary to +4500 V.

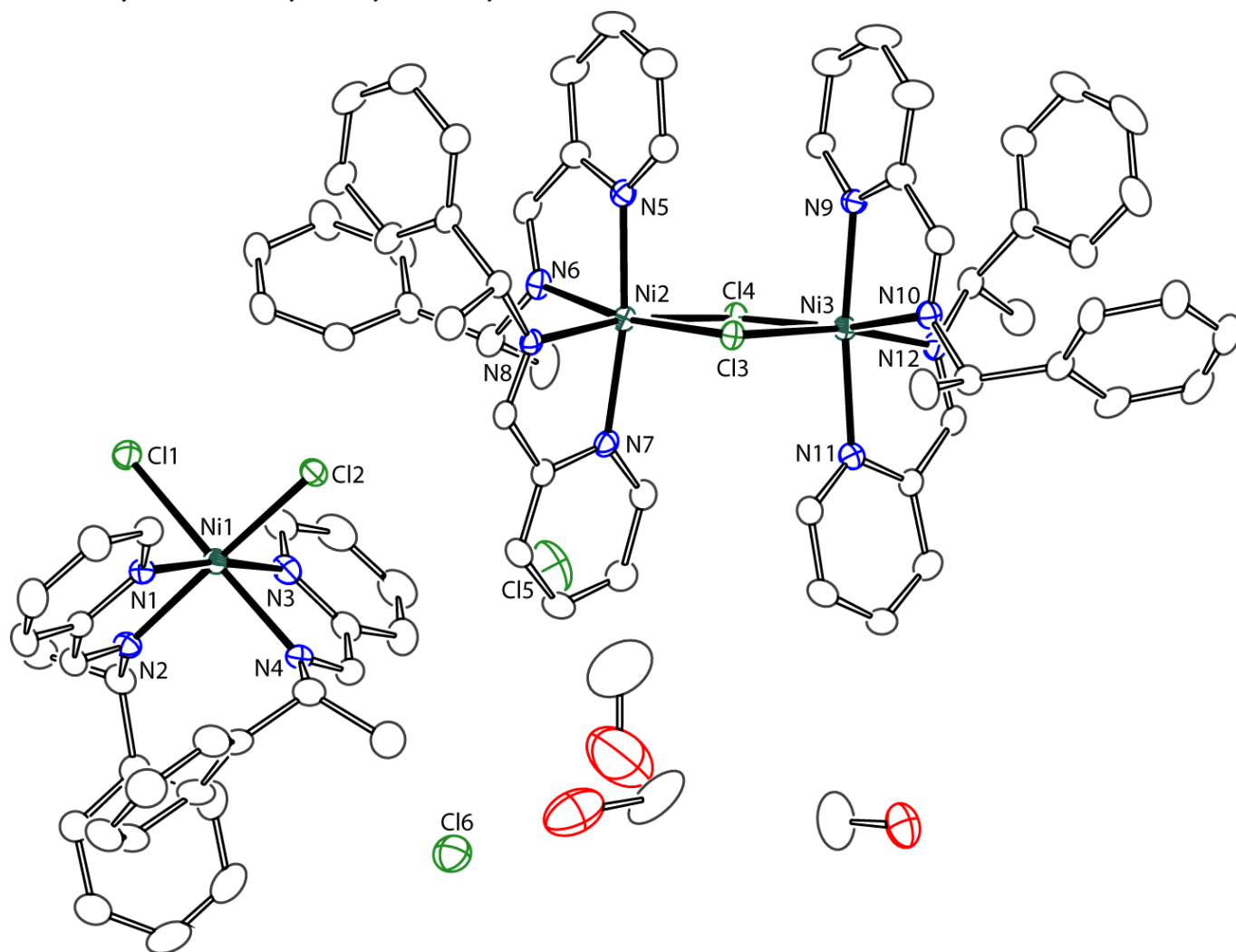


Figure S1. ORTEP drawing of $[\text{Ni}_2\text{Cl}_2(\text{L}^{\text{R}})_4][\text{NiCl}_2(\text{L}^{\text{R}})_2]\text{Cl}_2 \cdot 3\text{MeOH}$ (**1R**).

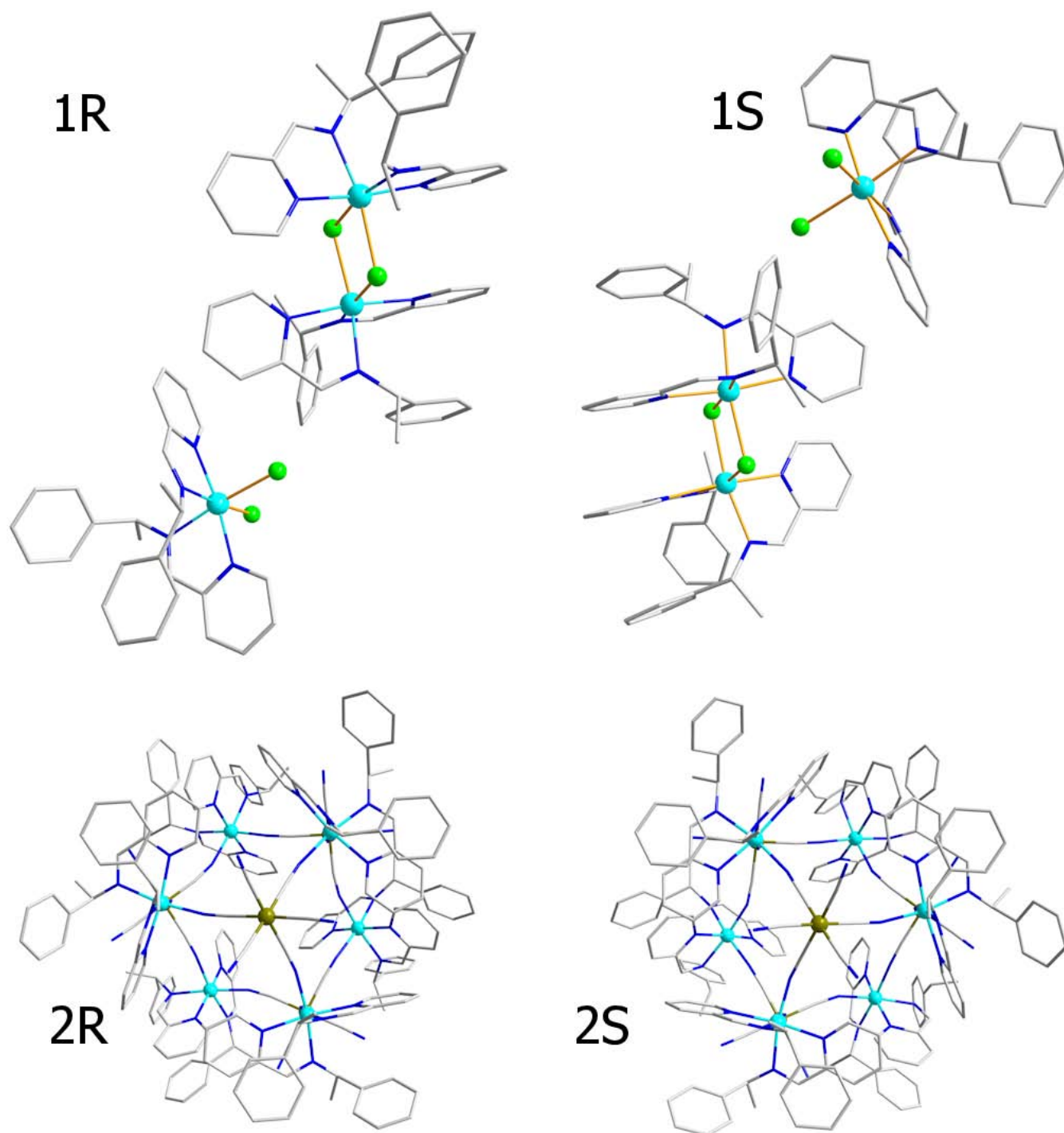


Figure S2. Structural comparison of 1R, 1S, 2R and 2S. All solvent molecules and counterions have been excluded for clarity.

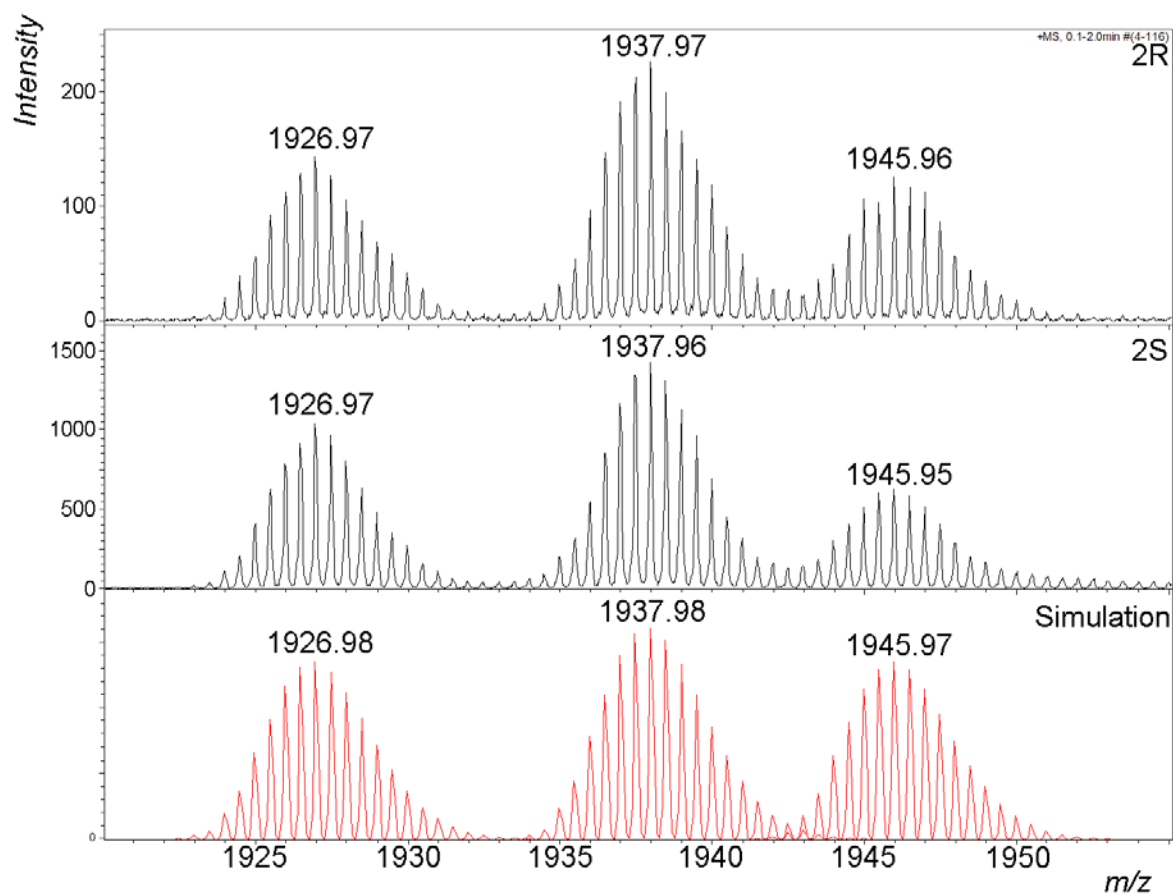


Figure S3. CSI-MS spectra of **2R** and **2S** observed (black) and simulated (red): 1926.98 = $[(Et_4N)H[Ni(L^{R/S})_2]_6[Fe(CN)_6]_4]^{2+}$; 1937.98 = $[(Et_4N)Na[Ni(L^{R/S})_2]_6[Fe(CN)_6]_4]^{2+}$; 1945.97 = $[(Et_4N)K[Ni(L^{R/S})_2]_6[Fe(CN)_6]_4]^{2+}$.

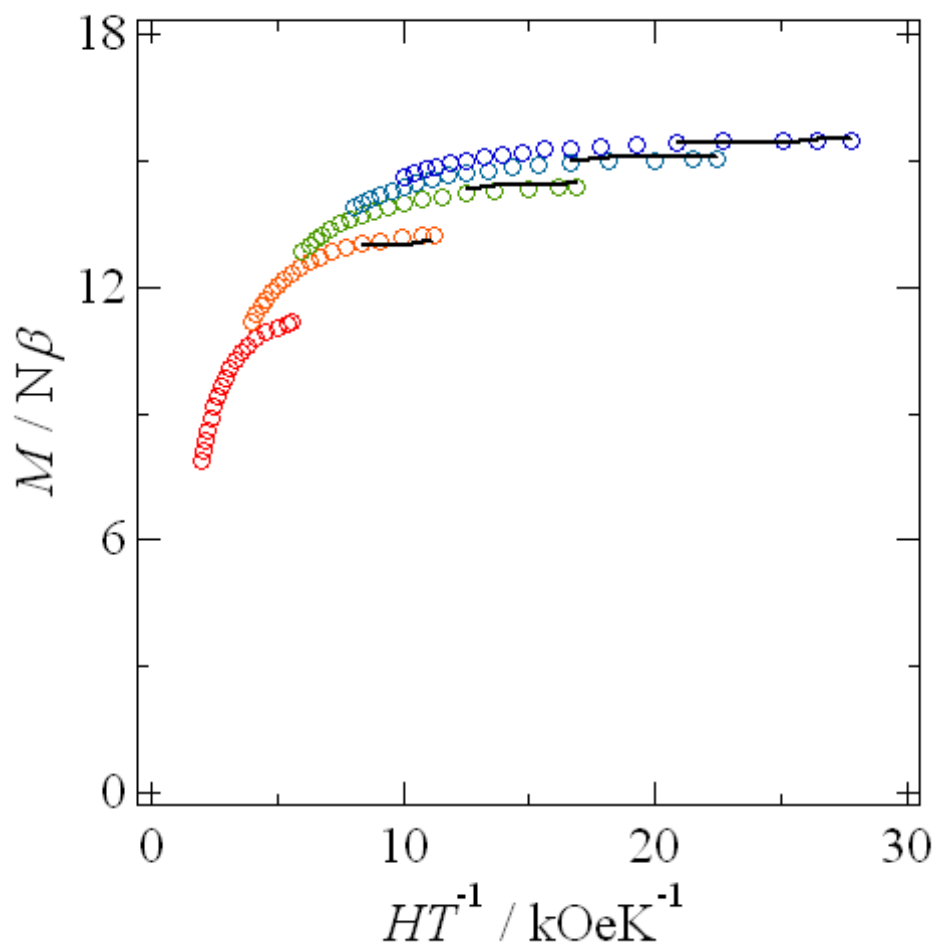


Figure S4. Plot of reduced magnetization ($M/N\beta$) versus H/T for **2R** in the temperature range 1.8 – 4.0 K and in applied fields of 1 – 5 T. Solid lines are the fit; see the text for the fitting parameters

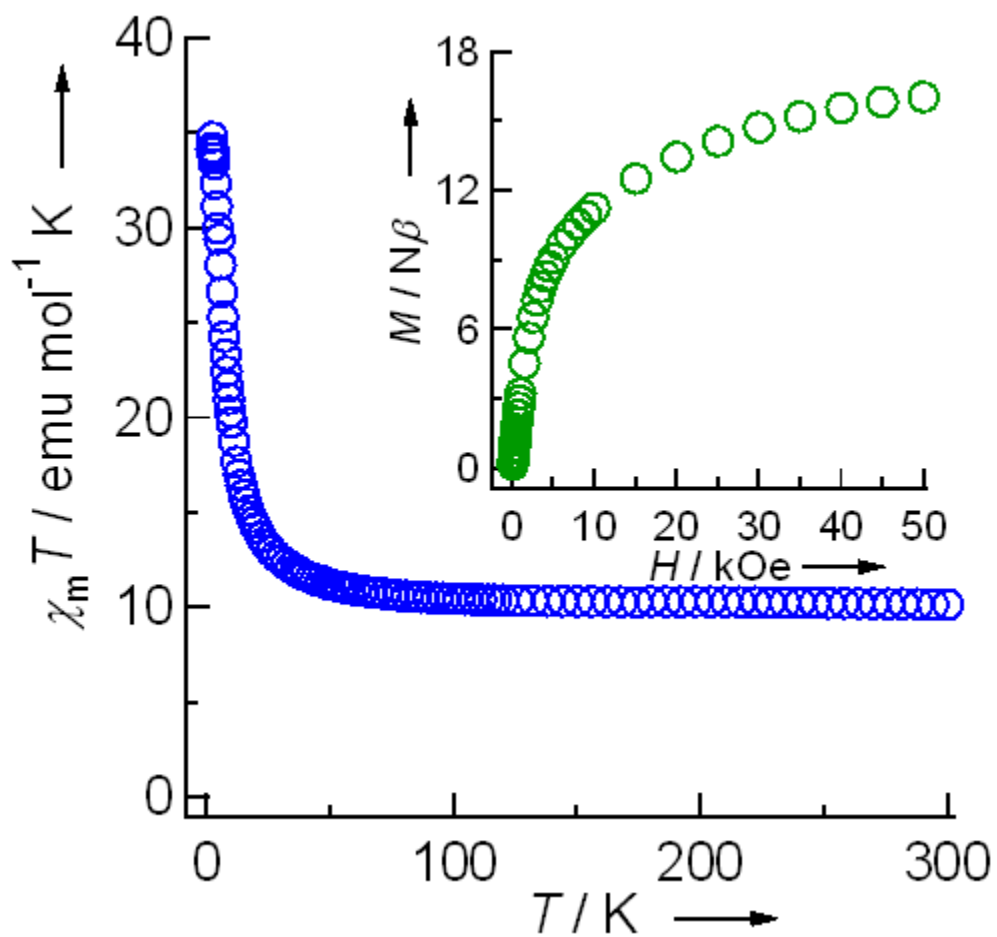


Figure S5. Plot of $\chi_m T$ vs. T of **2S** at applied field of 500 Oe. Inset: Field dependence of the magnetization at 1.8 K.

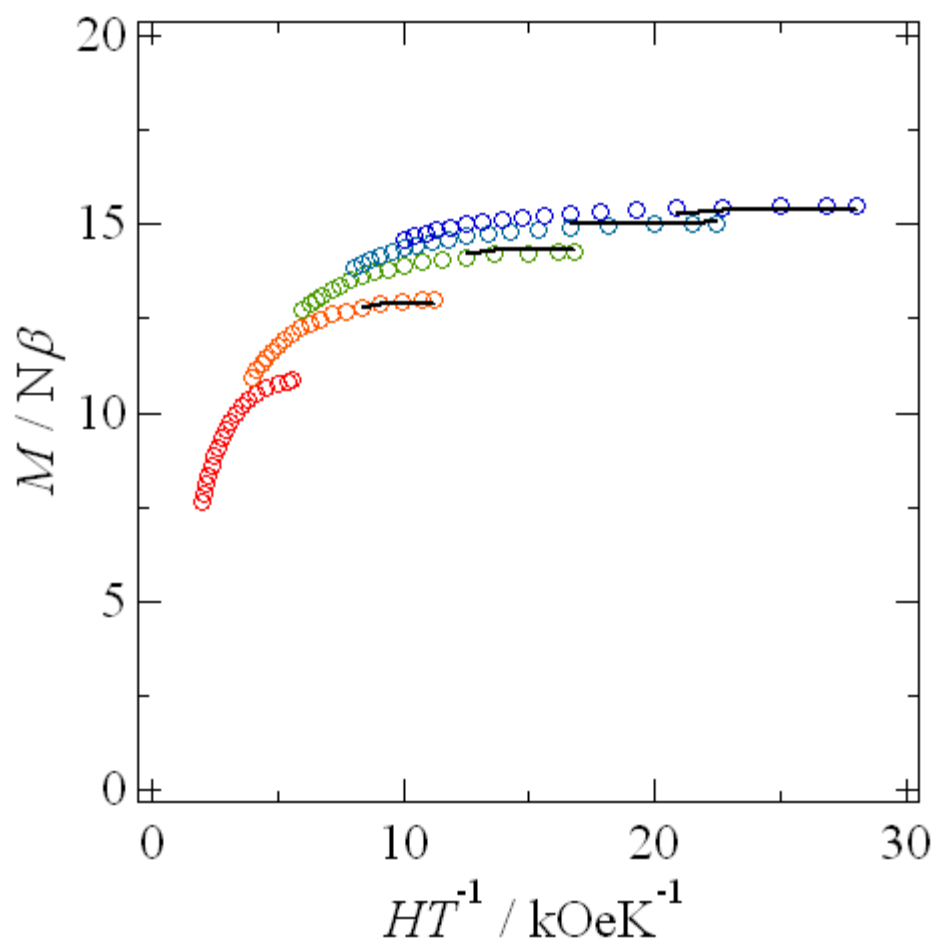


Figure S6. Plot of reduced magnetization ($M/N\beta$) versus H/T for **2S** in the temperature range 1.8 – 4.0 K and in applied fields of 1 – 5 T. Solid lines are the fit; see the text for the fitting parameters

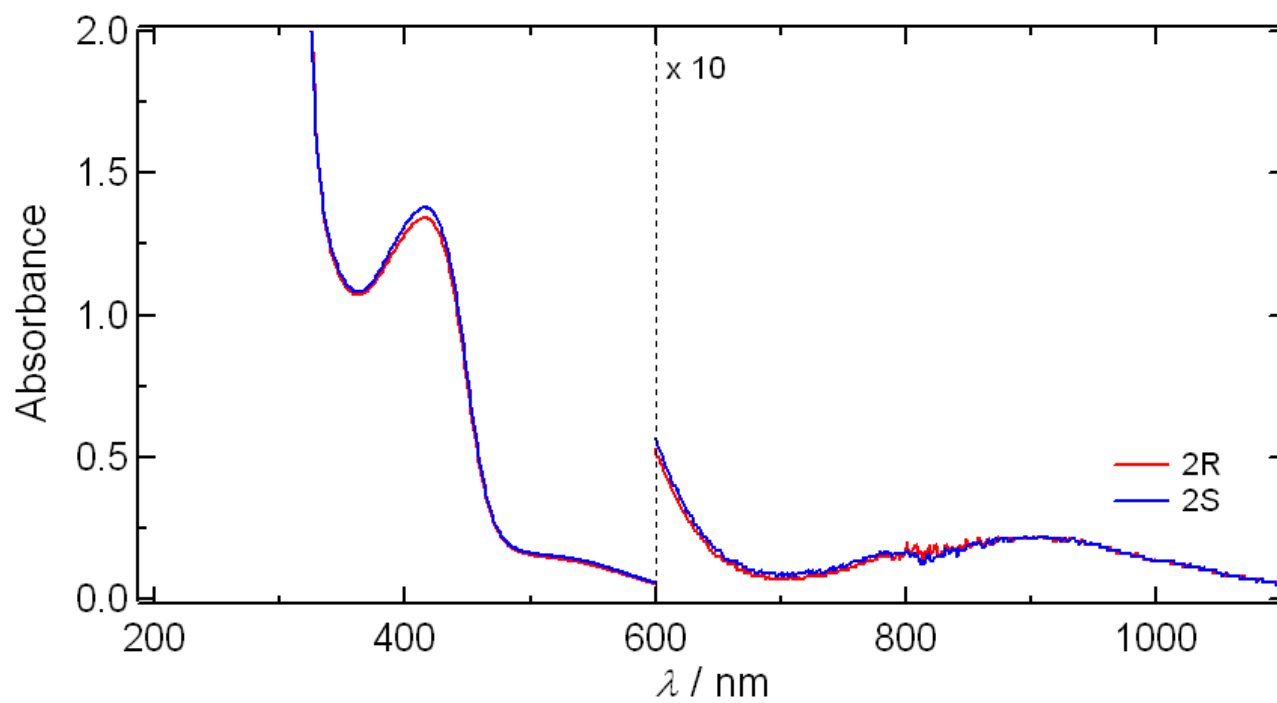


Figure S7. UV-vis spectra of **2R** and **2S**.

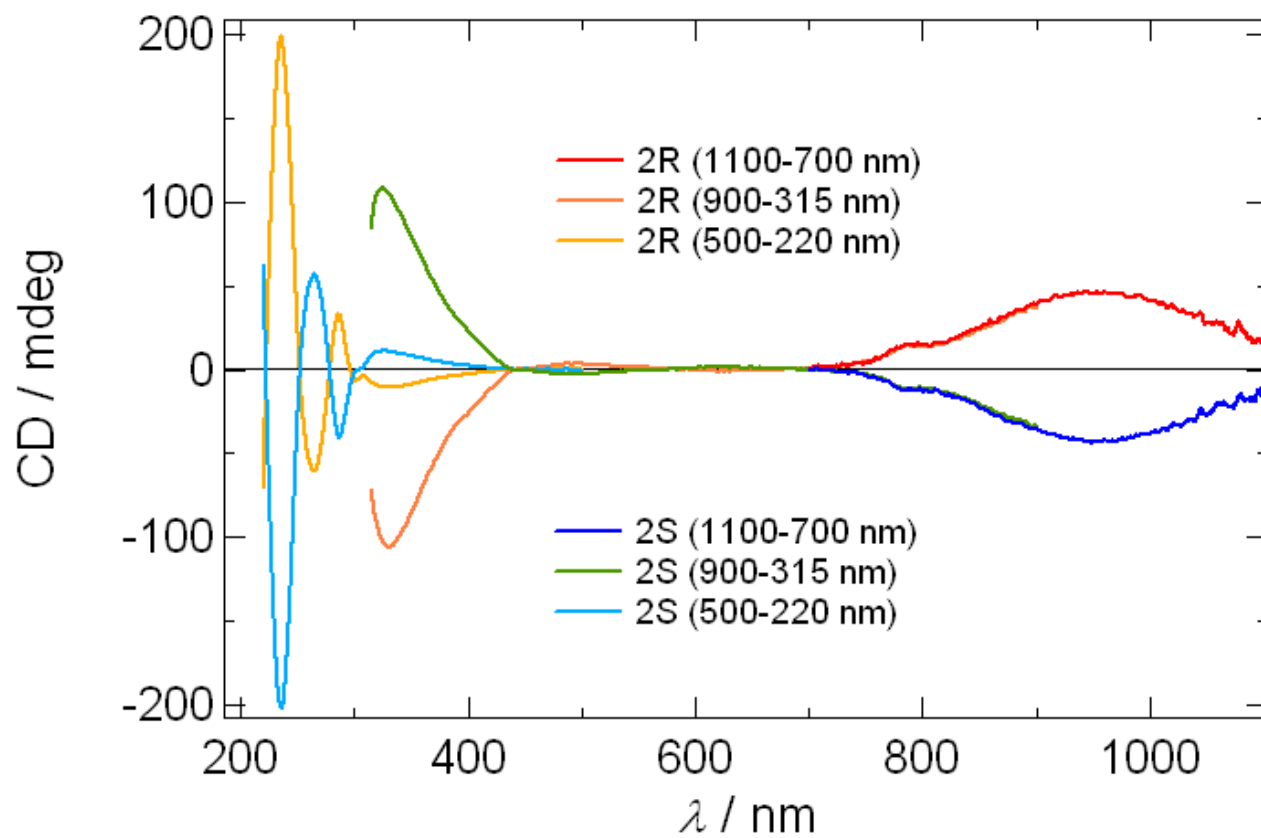


Figure S8. CD spectra of **2R** and **2S** in acetonitrile solution.